Materials Transactions, Vol. 49, No. 6 (2008) pp. 1346 to 1354

Electrochemical Iron-Chromium Alloying of Carbon Steel Surface Using Alternating Pulsed Electrolysis

Shunsuke Yagi[1,*], Hiroki Oshima[2], Kuniaki Murase[1], Eiichiro Matsubara[1] and Yasuhiro Awakura[1]

[1]*Department of Materials Science and Engineering, Kyoto University, Kyoto 606-8501, Japan*
[2]*Department of Materials Engineering, The University of Tokyo, Tokyo 113-8656, Japan*

Alternating pulsed electrolysis was investigated for the surface modification of carbon steel substrates with carbon contents of 0.2 mass%, 0.6 mass% and 0.8 mass%. This process involves the anodic periodic dissolution of substrates to provide ferrous or ferric ions near the substrate as an electroactive component to form the objective alloy during subsequent cathodic times. The carbon steel substrates dissolved heterogeneously since the substrates had nonuniform texture composed of ferrite, cementite, and pearlite. Although the heterogeneous dissolution tended to provide a rough surface of the iron-chromium alloy layers, which resulted in poor adhesion of the layers, relatively flat and smooth alloy layers were obtained by reducing the amount of dissolved iron during each anodic pulse. Pits and defects that were originally recognized on the carbon steel substrate were gradually filled in and covered with iron-chromium alloy by the pulsed electrolysis.
[doi:10.2320/matertrans.MRA2008028]

(Received January 21, 2008; Accepted March 12, 2008; Published April 23, 2008)

Keywords: *surface modification, carbon steel, iron-chromium alloying, alternating pulsed electrolysis*

1. Introduction

Metallic chromium is galvanized on many kinds of industrial parts including, for example, automotive wheels, fenders, and trims, as well as articles for daily use such as steel office furniture, faucets, and golf clubs. This is because the electroplating of chromium is an inexpensive and effective way to provide good properties, *i.e.* brilliance, hardness, abrasion resistance, and corrosion resistance to substrate materials. In 1856, Geuther succeeded in the first electrodeposition of chromium from an aqueous solution containing hexavalent chromate compound,[1,2] and the chromium plating bath based on chromate compound was then established in 1920; the bath is known as the famous Sargent bath at present.[3] Thereafter, a constant effort has been made to improve the chromium plating bath, and many kinds of plating baths based on the Sargent bath have been put to practical use for many years.[4–8] Among the many efforts, electrolysis with a pulsed current has been reported to improve the surface appearance and mechanical properties of chromium layers[9,10] or chromium alloy layers.[11,12]

The European Parliament issued a directive on restrictions of hazardous substances (RoHS directive 2002/95/EC) in January 27, 2003, and thereafter the trend to eliminate the usage of hexavalent chromium compounds has spread throughout the field of chromium plating in the world. Against the background, many alternative chromate-free techniques have been investigated. One of the most eagerly anticipated alternatives is chromium electroplating based on aqueous solutions containing divalent chromium ions (Cr(II))[13] or trivalent chromium ions (Cr(III)).[14–18] Specifically, chromium electroplating from aqueous solutions containing trivalent chromium ions, *i.e.* chromic ions, is a promising candidate. However, it is difficult to electroplate a thick metallic chromium layer from chromic solutions. Furthermore, it is known that the chromium layer electrodeposited from the chromic solutions has different properties from the chromium layer electrodeposited conventionally from aqueous chromate solutions. For example, the former has higher values of carbon and oxygen contents than the latter and is thus brittle and tends to fracture, resulting in cracks. Cracks on the substrate surface may cause the depression in corrosion resistance since liquid gets through the niches.

To overcome the drawbacks associated with conventional chromium plating processes, we have investigated an iron-chromium alloying of a four-nine pure iron substrate surface as a novel surface modification technology using a trivalent chromium solution by alternating pulsed electrolysis.[19,20] The deposited iron-chromium layers had a continuous composition gradient, showing good adhesion, and no cracks were observed on the surface of the layers. Pure iron substrate is, however, not practical compared to conventional carbon steel, and hence it is worth examining whether alternating pulsed electrolysis is applicable to the surface alloying of carbon steel substrates. In the present work, iron-chromium alloying on the surface of conventional carbon steel was examined by alternating pulsed electrolysis in terms of substrate texture, anodic dissolution behavior, and cathodic alloy formation.

In alternating pulsed electrolysis, the plating baths employed for the electrolysis contain only a chromic salt as the electroactive metal ion component, while at least two electroactive metal ion components are present in conventional alloy electrolysis. Therefore, another metal component, *i.e.* ferrous or ferric ion, is provided in the plating solution near the substrate through the dissolution of the iron substrate during the periods of anodic polarization (anodic pulse time t_a) in alternating pulsed electrolysis. Iron-chromium alloy is then electrodeposited on the substrate during the subsequent periods of cathodic polarization (cathodic pulse time t_c). With multiple cycles of alternating

*Corresponding author, E-mail: syagi@mtl.kyoto-u.ac.jp

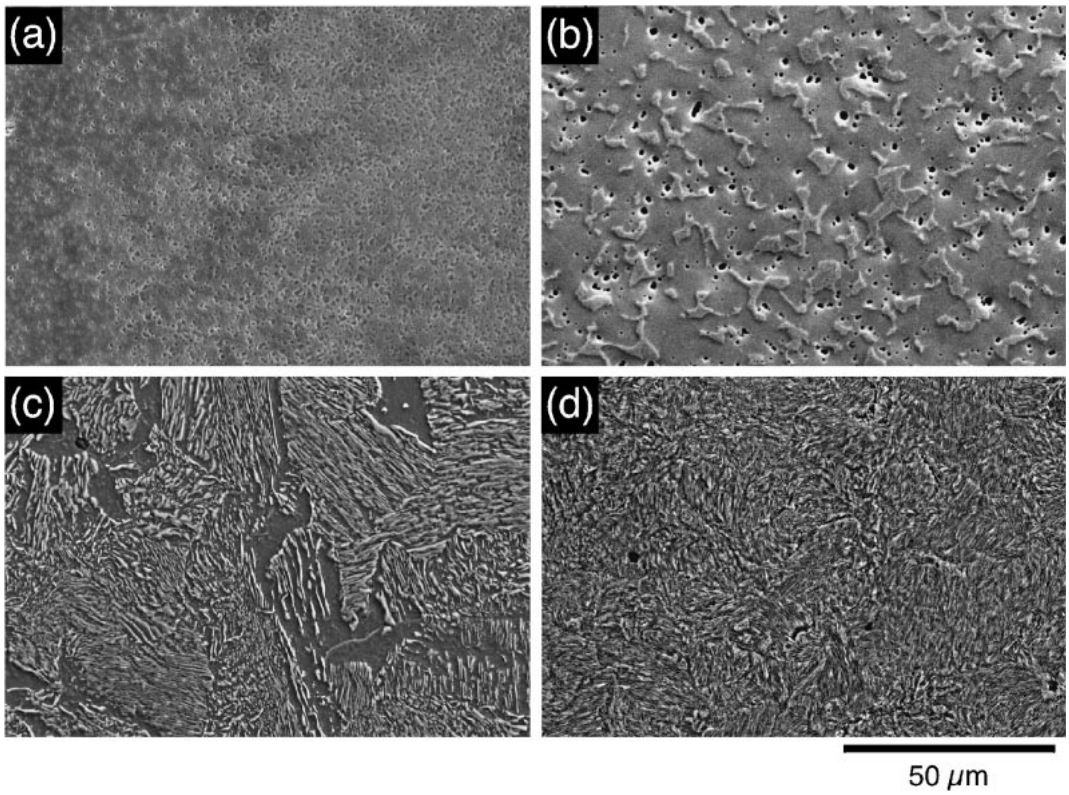

Fig. 1 Surface SEM images of (a) four-nine pure iron and (b) 0.2 mass%C, (c) 0.6 mass%C, (d) 0.8 mass%C steel substrates etched in an aqueous solution of C_2H_5OH and HNO_3 for 5 s.

pulsed electrolysis, the iron substrate is gradually covered with a stable iron-chromium alloy layer, and finally, a thin layer of iron-chromium alloy is developed on the whole surface of the iron substrate. After a continuous iron-chromium layer coats the entire surface, the dissolution of the iron substrate no longer occurs and chromium only deposits. Carbon steel substrates are different in composition and texture from pure iron, and these differences may affect the dissolution behavior.

2. Experimental

An acidic aqueous solution of 0.10 kmol m^{-3} $Cr_2(SO_4)_3$ - 1.0 kmol m^{-3} KCl - 0.65 kmol m^{-3} H_3BO_3 - 1.0 kmol m^{-3} NH_4Cl - 1.0 kmol m^{-3} HCOOK[21] was used for alternating pulsed electrolysis. All chemicals were of reagent grade and were used without any pretreatment. The deionized water to dissolve the chemicals had a specific resistance greater than $5 \times 10^6\ \Omega$ cm. The pH of the solution was adjusted to 2.4 using hydrochloric acid aqueous solution. Electrolytes aged for more than 24 hours were used to obtain reproducible results. Electrolysis was performed at room temperature in 250 cm^3 of plating solution in a Pyrex beaker 300 cm^3 in capacity using a conventional three-electrode setup. Pure iron plates with four-nine purity and carbon steel (0.2 mass%C–0.8 mass%C) plates measuring 7.1 mm on each side were cemented in epoxy resin so that one surface was exposed to the solution, and were used as working electrodes. A platinum plate measuring 20 × 20 mm was used as a counter electrode. A Ag/AgCl electrode immersed in a 3.33 kmol m^{-3} KCl aqueous solution was used as a reference (+0.206 V *vs.* SHE); the potentials were recalculated for the standard hydrogen electrode (SHE). During electrolysis, the solution was agitated at a rate of 640 rpm with a magnetic stirring unit. The surface morphology of the resulting layers was observed with a scanning electron microscope (SEM). The layer composition was estimated by X-ray fluorescence analysis (XRF).

3. Results and Discussion

3.1 Relation between dissolution behavior and substrate texture

Pure iron substrate has only a ferrite texture, while carbon steel substrate without heat treatment has ferrite, cementite and pearlite textures.[22] The dissolution behaviors of these substrates can be different from each other, depending on the texture of the substrates. Figure 1 shows the surface SEM images of four-nine pure iron and 0.2 mass%C–0.8 mass%C steel substrates, which were etched in a mixed solution of C_2H_5OH and HNO_3 for 5 s. The 0.2 mass%C steel substrate had an island-like cementite texture in ferrite matrix, and many pits were observed on the surface. The 0.6 mass%C steel substrate consisted of a complicated ferrite and pearlite texture; pearlite is a lamella texture of ferrite and cementite phases. The whole surface of the 0.8 mass%C steel substrate consisted mainly of pearlite.

The pure iron substrate was heat-treated at 800°C for 1 hour to observe the dissolution behavior in detail. The heat-treated iron substrate was anodically dissolved at 0.0 V *vs.* SHE for 1 min–10 min in the same solution as for alternating pulsed electrolysis. Figure 2 shows the surface SEM images

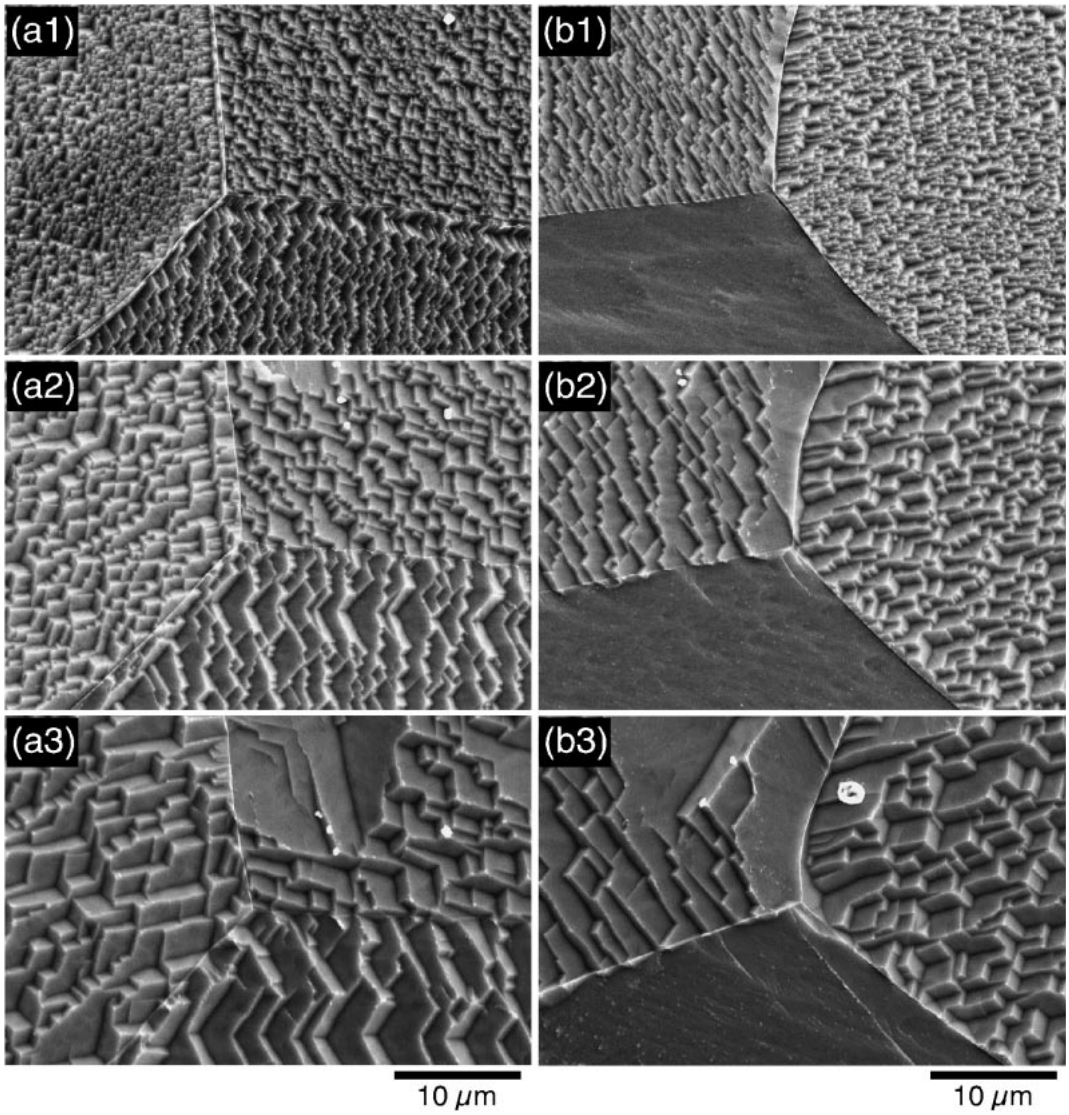

Fig. 2 Surface SEM images of four-nine pure iron dissolved at 0.0 V *vs.* SHE for (a1) and (b1) 1 min, (a2) and (b2) 5 min, (a3) and (b3) 10 min, in an aqueous solution (pH 2.4) containing 0.10 kmol m^{-3} $Cr_2(SO_4)_3$, 1.0 kmol m^{-3} KCl, 0.65 kmol m^{-3} H_3BO_3, 1.0 kmol m^{-3} NH_4Cl, and 1.0 kmol m^{-3} HCOOK.

of the heat-treated pure iron substrates after the dissolution process. Dissolution proceeded on the whole surface independently of dissolution time remaining in particular planes of crystal grains, which should be close-packed planes of iron with bcc structure, *i.e.* 110 planes.[23] Orientation was different among these crystal grains, and some grains eventually exposed the 110 plane on their surfaces, showing a flat surface as in series (b) in Fig. 2. The dissolution behavior was also different at each grain and was not microscopically uniform. However, the dissolution was macroscopically uniform since the dissolution current was almost constant for 10 min as can be seen in Fig. 3.

Figure 4 shows surface SEM images of carbon steel substrates after the anodic dissolution at 0.0 V *vs.* SHE for 10 min. Cementite was insoluble and remained on the substrate, and the amount increased with an increase in the carbon content. The surface of the 0.8 mass%C steel substrate was flatter than that of the 0.2 mass%C steel substrate after the anodic dissolution because the whole surface of the 0.8 mass%C steel substrate was covered with pearlite.

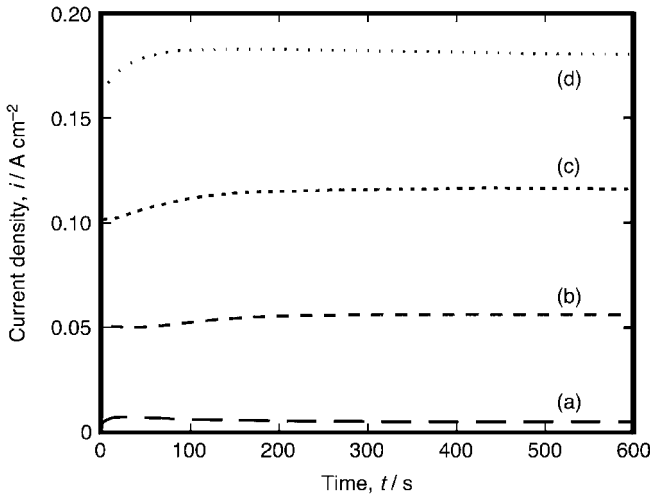

Fig. 3 Current densities for the anodic dissolution of a heat-treated pure iron substrate at (a) −0.2 V, (b) −0.1 V, (c) 0.0 V, and (d) 0.1 V *vs.* SHE for 10 min in an aqueous solution (pH 2.4) containing 0.10 kmol m^{-3} $Cr_2(SO_4)_3$, 1.0 kmol m^{-3} KCl, 0.65 kmol m^{-3} H_3BO_3, 1.0 kmol m^{-3} NH_4Cl, and 1.0 kmol m^{-3} HCOOK.

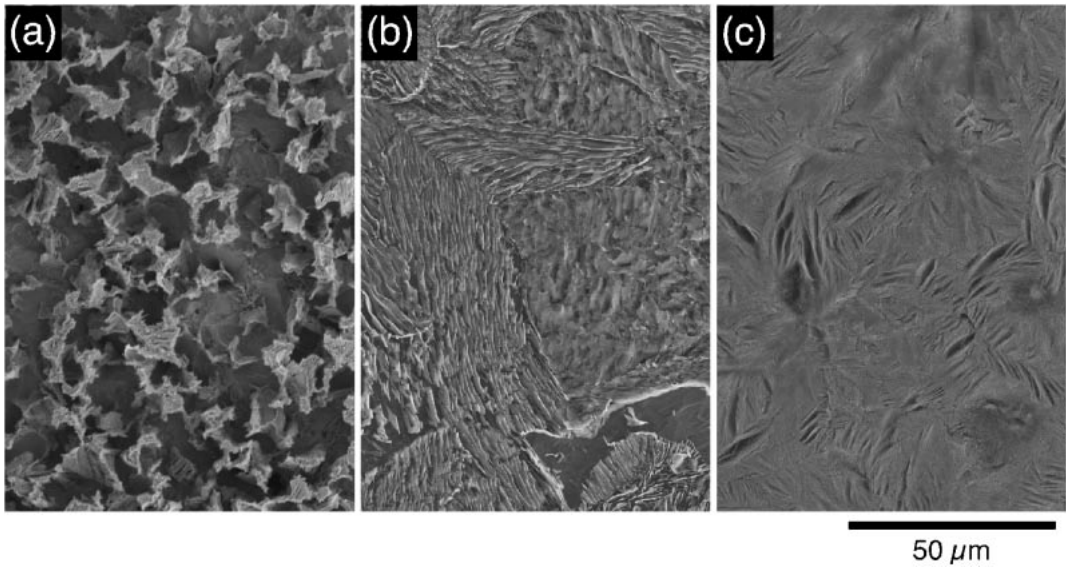

Fig. 4 Surface SEM images of (a) 0.2 mass%C, (b) 0.6 mass%C, and (c) 0.8 mass%C steel substrates after the dissolution at 0.0 V *vs.* SHE for 10 min in an aqueous solution (pH 2.4) containing 0.10 kmol m^{-3} $Cr_2(SO_4)_3$, 1.0 kmol m^{-3} KCl, 0.65 kmol m^{-3} H_3BO_3, 1.0 kmol m^{-3} NH_4Cl, and 1.0 kmol m^{-3} HCOOK.

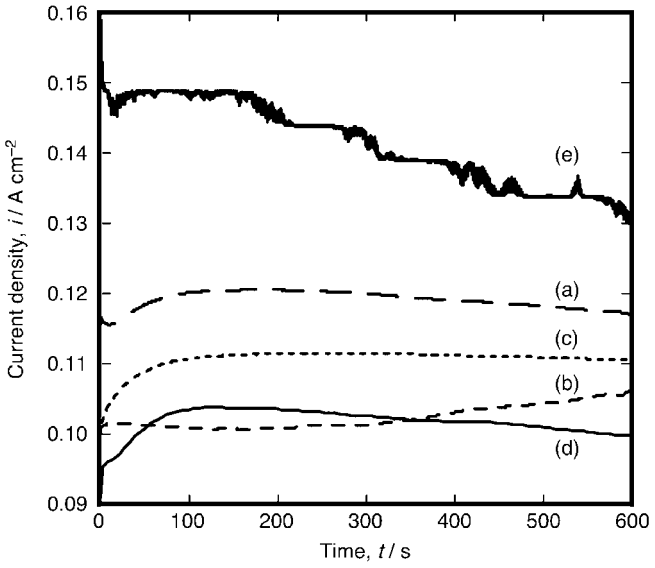

Fig. 5 Current densities for the anodic dissolution of (a) four-nine pure iron (before heat treatment), (b) four-nine pure iron (after heat treatment), (c) 0.2 mass%C, (d) 0.6 mass%C, and (e) 0.8 mass%C steel substrates at 0.0 V *vs.* SHE for 10 min in an aqueous solution (pH 2.4) containing 0.10 kmol m^{-3} $Cr_2(SO_4)_3$, 1.0 kmol m^{-3} KCl, 0.65 kmol m^{-3} H_3BO_3, 1.0 kmol m^{-3} NH_4Cl, and 1.0 kmol m^{-3} HCOOK.

Figure 5 shows that the anodic dissolution current densities of (d) 0.6 mass%C and (e) 0.8 mass%C steel substrates decreased gradually with time, indicating that soluble ferrite was preferentially dissolved and insoluble cementite was left. Thus, also in alternating pulsed electrolysis, too much dissolution of substrates may cause the nonuniformity of the surface, resulting in poor adhesion of the deposited layer or cracks and fractures in the layer.

3.2 Alternating pulsed electrolysis for iron-chromium alloying on conventional carbon steel

Iron-chromium alloying on the surfaces of the carbon steel substrates was examined by alternating pulsed electrolysis. It is possible that iron-chromium layers of less than 1 μm in thickness are formed on iron substrates by alternating pulsed electrolysis as we reported.[19,20] Figure 6 shows the surface SEM images of the 0.8 mass%C steel substrates before and after the process for 10 min by pulsed electrolysis under three conditions; $E_c = -1.1$ V, $E_a = 0.0$ V, $t_c = 2.00$ s, and $t_a = 0.25$ s, 0.50 s, 1.00 s. The deposited layers were all nonuniform and detachment was observed on all the surfaces. This ununiformity arises from the substrate texture, resulting in poor adhesion between the deposited layers and the substrate. In contrast, flat and adhesive iron-chromium layers are formed on a pure iron substrate under the same conditions.[19,20]

In order to reduce the effects of texture, the cathodic pulse time t_c was increased to 4.00 s and pulsed electrolysis was performed again; the total cathodic pulse time was kept constant at 10 min, and so the total of the anodic pulse time was decreased by half. As shown in Fig. 7, however, the surface was not improved so much and the peeled area increased with increasing t_a. The amount of chromium in the deposited layer was increased with increases in both t_c and t_a as plotted in Fig. 8 except for the substrate processed at $t_c = 4.00$ s, $t_a = 1.00$ s. This suggests that chromium deposition was stimulated by ferrous or ferric ions dissolved in the vicinity of the substrate. The anodic pulse potential E_a was then decreased to −0.1 V *vs.* SHE in order to depress the dissolution slightly, and pulsed electrolysis was performed under the same conditions except for E_a. Figure 9 shows the surface SEM images of the substrate surfaces, where flat and continuous layers were observed on all the substrate surfaces. The number of pits on the layer seemed to increase with the increase in t_a just as mentioned above, and the layer obtained at $t_a = 0.25$ s was the most uniform among those at the other t_a. Figure 10 indicates that the amount of chromium in the layer was almost the same in the t_a range of 0.50 s to 1.00 s, while it increased with increasing t_a in the range of 0.25 s to

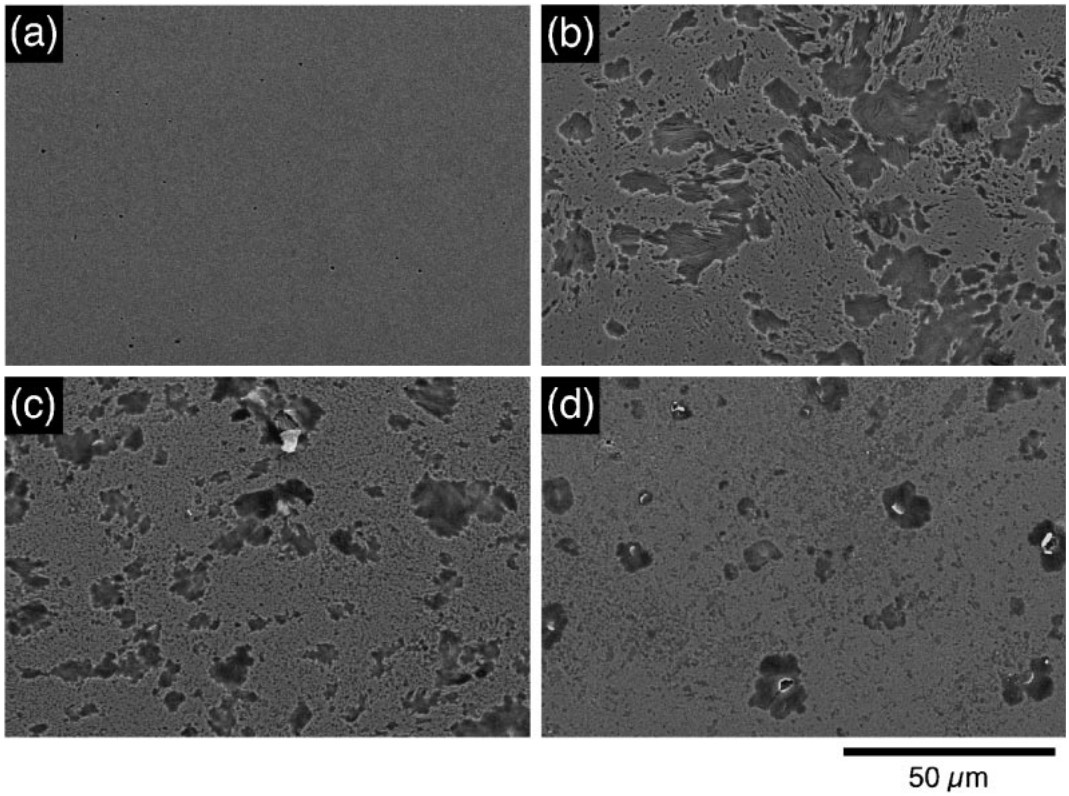

Fig. 6 Surface SEM images of a 0.8 mass%C steel substrate (a) before processing, and 0.8 mass%C steel substrates processed by alternating pulsed electrolysis for 300 pulse cycles under the conditions: $E_c = -1.1$ V *vs.* SHE, $E_a = 0.0$ V *vs.* SHE, $t_c = 2.00$ s, and $t_a =$ (b) 0.25 s, (c) 0.50 s, (d) 1.00 s in an aqueous solution (pH 2.4) containing 0.10 kmol m^{-3} $Cr_2(SO_4)_3$, 1.0 kmol m^{-3} KCl, 0.65 kmol m^{-3} H_3BO_3, 1.0 kmol m^{-3} NH_4Cl, and 1.0 kmol m^{-3} HCOOK.

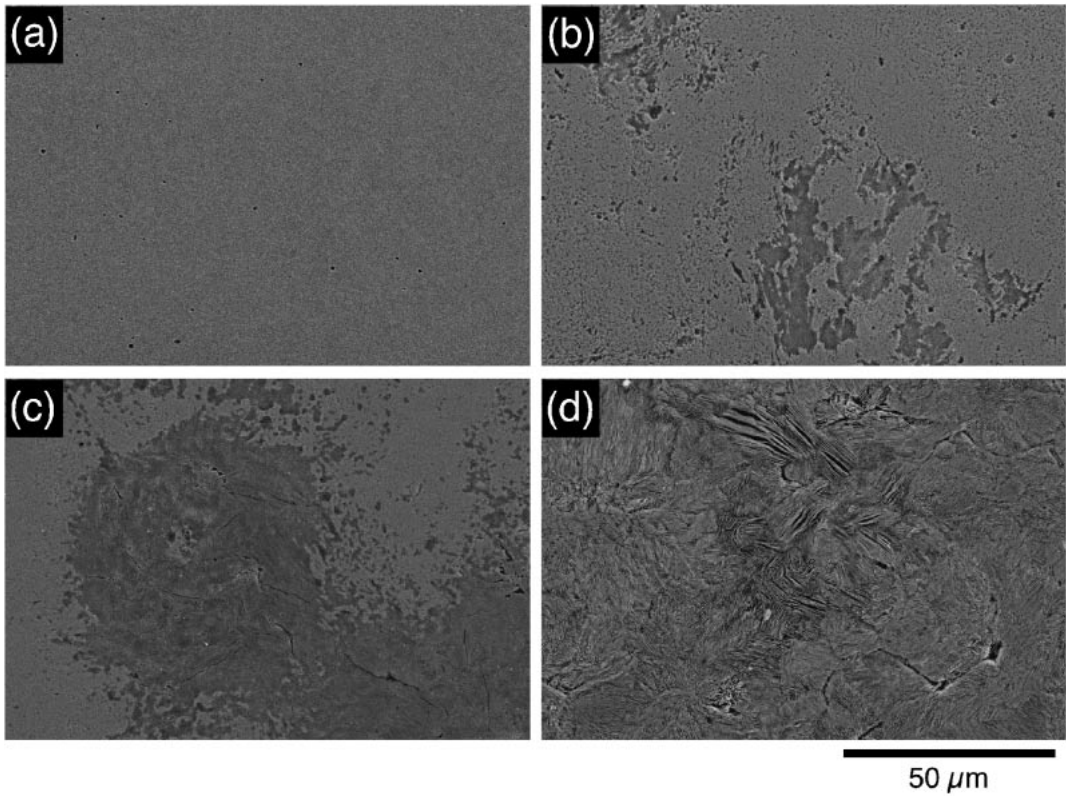

Fig. 7 Surface SEM images of a 0.8 mass%C steel substrate (a) before processing and 0.8 mass%C steel substrates processed by alternating pulsed electrolysis for 150 pulse cycles under the conditions: $E_c = -1.1$ V *vs.* SHE, $E_a = 0.0$ V *vs.* SHE, $t_c = 4.00$ s, and $t_a =$ (b) 0.25 s, (c) 0.50 s, (d) 1.00 s in an aqueous solution (pH 2.4) containing 0.10 kmol m^{-3} $Cr_2(SO_4)_3$, 1.0 kmol m^{-3} KCl, 0.65 kmol m^{-3} H_3BO_3, 1.0 kmol m^{-3} NH_4Cl, and 1.0 kmol m^{-3} HCOOK.

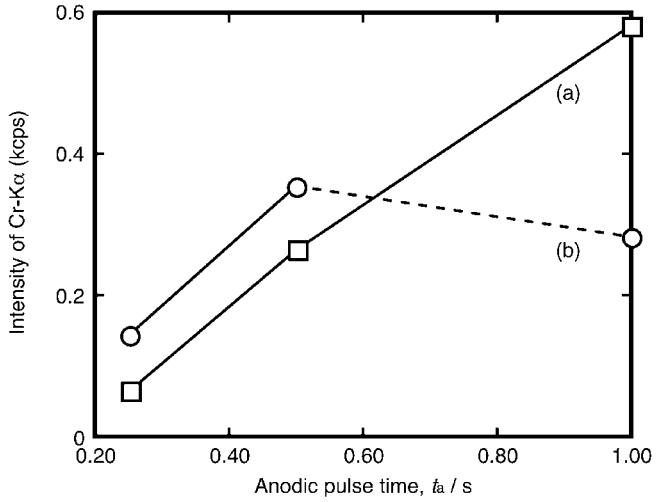

Fig. 8 Cr-Kα intensities of layers formed on 0.8 mass%C steel substrates by alternating pulsed electrolysis from an aqueous solution (pH 2.4) containing 0.10 kmol m^{-3} $Cr_2(SO_4)_3$, 1.0 kmol m^{-3} KCl, 0.65 kmol m^{-3} H_3BO_3, 1.0 kmol m^{-3} NH_4Cl, and 1.0 kmol m^{-3} HCOOK under the conditions: $E_c = -1.1$ *vs.* SHE, $E_a = 0.0$ V *vs.* SHE, $t_c =$ (a) 2.00 and (b) 4.00 s, $t_a = 0.25$ s–1.00 s.

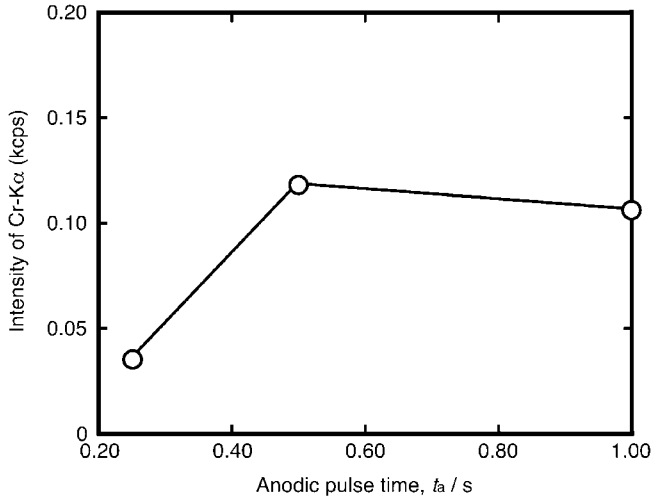

Fig. 10 Cr-Kα intensities of layers formed on 0.8 mass%C steel substrates by alternating pulsed electrolysis from an aqueous solution (pH 2.4) containing 0.10 kmol m^{-3} $Cr_2(SO_4)_3$, 1.0 kmol m^{-3} KCl, 0.65 kmol m^{-3} H_3BO_3, 1.0 kmol m^{-3} NH_4Cl, and 1.0 kmol m^{-3} HCOOK under the conditions: $E_c = -1.1$ *vs.* SHE, $E_a = -0.1$ V *vs.* SHE, $t_c = 4.00$ s, $t_a = 0.25$ s–1.00 s.

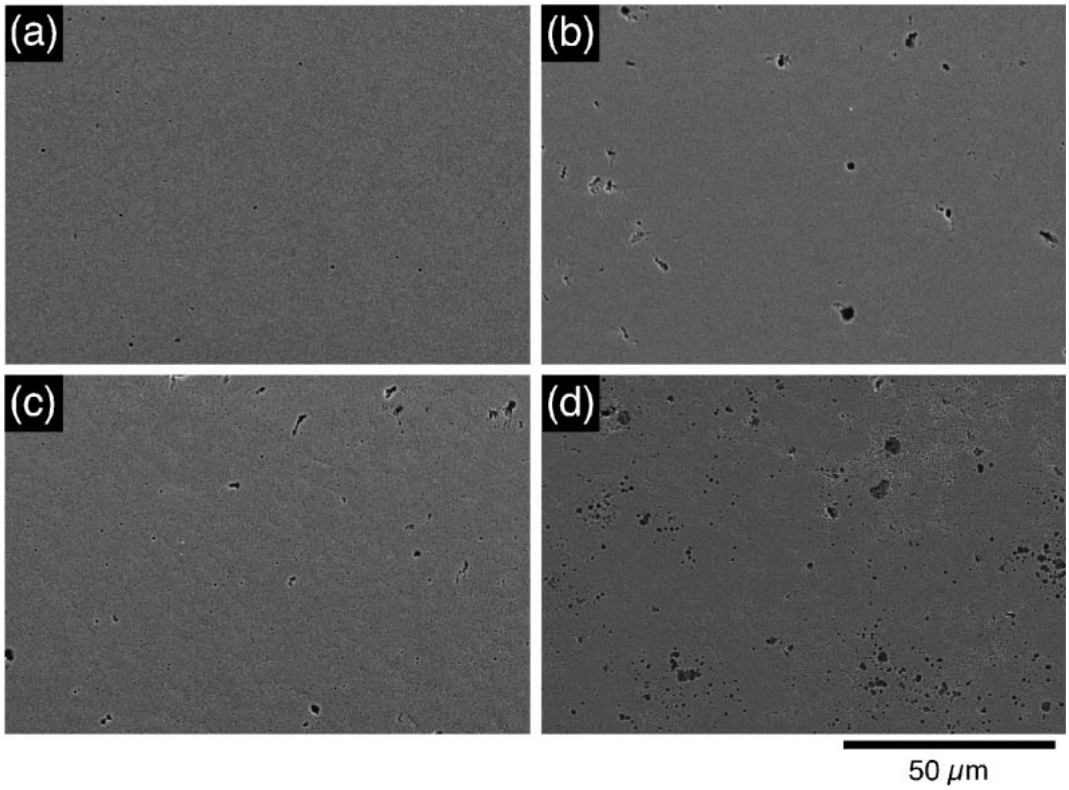

Fig. 9 Surface SEM images of a 0.8 mass%C steel substrate (a) before processing and 0.8 mass%C steel substrates processed by alternating pulsed electrolysis for 150 pulse cycles under the conditions: $E_c = -1.1$ V *vs.* SHE, $E_a = -0.1$ V *vs.* SHE, $t_c = 4.00$ s, and $t_a =$ (b) 0.25 s, (c) 0.50 s, (d) 1.00 s in an aqueous solution (pH 2.4) containing 0.10 kmol m^{-3} $Cr_2(SO_4)_3$, 1.0 kmol m^{-3} KCl, 0.65 kmol m^{-3} H_3BO_3, 1.0 kmol m^{-3} NH_4Cl, and 1.0 kmol m^{-3} HCOOK.

0.50 s. This is because the number of pits increased with the increase in anodic pulse time although the increase in anodic pulse time resulted in an increase in the concentration of ferrous or ferric ions near the substrate, which stimulates chromium deposition. Figure 11 shows the current density transients during alternating pulsed electrolysis for 100 s under the conditions: (a) $E_c = -1.1$ V *vs.* SHE, $E_a = 0.0$ V *vs.* SHE, $t_c = 2.00$ s, $t_a = 0.50$ s, (b) $E_c = -1.1$ V *vs.* SHE, $E_a = 0.0$ V *vs.* SHE, $t_c = 4.00$ s, $t_a = 0.50$ s, (c) $E_c = -1.1$ V *vs.* SHE, $E_a = -0.1$ V *vs.* SHE, $t_c = 4.00$ s, $t_a = 0.50$ s. Under condition (a), the anodic current density drastically decreased with time and became almost constant after the

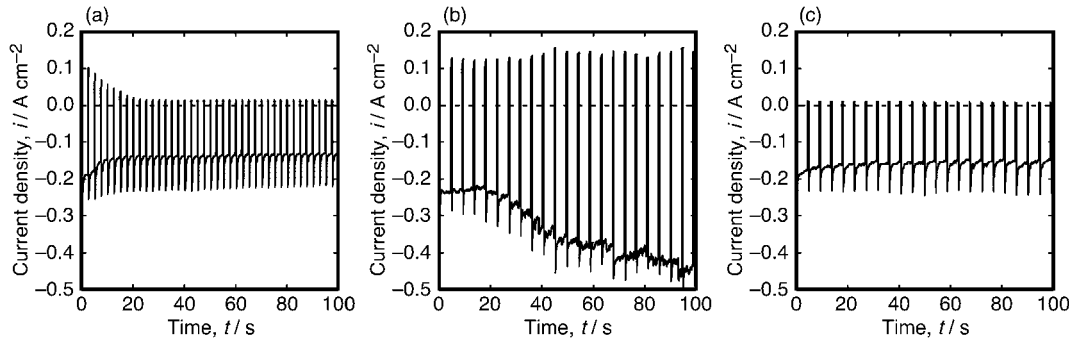

Fig. 11 Current density transient during alternating pulsed electrolysis for 100 s under the conditions: (a) $E_c = -1.1$ V *vs.* SHE, $E_a = 0.0$ V *vs.* SHE, $t_c = 2.00$ s, $t_a = 0.50$ s, (b) $E_c = -1.1$ V *vs.* SHE, $E_a = 0.0$ V *vs.* SHE, $t_c = 4.00$ s, $t_a = 0.50$ s, (c) $E_c = -1.1$ V *vs.* SHE, $E_a = -0.1$ V *vs.* SHE, $t_c = 4.00$ s, $t_a = 0.50$ s in an aqueous solution (pH 2.4) containing 0.10 kmol m^{-3} $Cr_2(SO_4)_3$, 1.0 kmol m^{-3} KCl, 0.65 kmol m^{-3} H_3BO_3, 1.0 kmol m^{-3} NH_4Cl, and 1.0 kmol m^{-3} HCOOK.

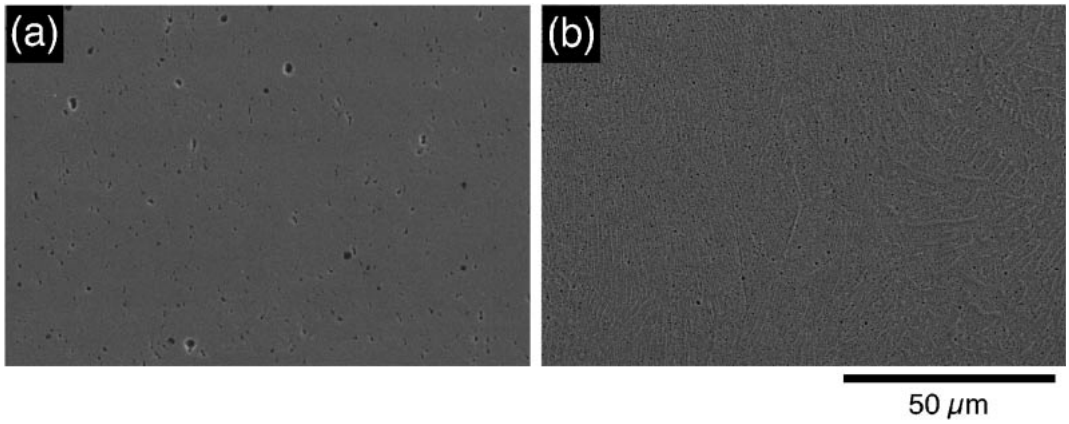

Fig. 12 Surface SEM images of (a) 0.2 mass%C and (b) 0.6 mass%C steel substrates processed by alternating pulsed electrolysis for 150 pulse cycles under the conditions: $E_c = -1.1$ V *vs.* SHE, $E_a = -0.1$ V *vs.* SHE, $t_c = 4.00$ s, and $t_a = 0.25$ s in an aqueous solution (pH 2.4) containing 0.10 kmol m^{-3} $Cr_2(SO_4)_3$, 1.0 kmol m^{-3} KCl, 0.65 kmol m^{-3} H_3BO_3, 1.0 kmol m^{-3} NH_4Cl, and 1.0 kmol m^{-3} HCOOK.

10th cycle, while the cathodic current density was slightly decreased with time. This indicates that the soluble ferrite on the surface was preferentially dissolved in the early pulse cycles and the insoluble cementite remained on the surface by intensive anodic polarization. Under condition (b), the anodic current density was almost steady, but the cathodic current density gradually increased with time, suggesting an increase in the surface area by the excessive dissolution of a substrate or deposited iron-chromium alloy with low chromium content. In contrast, under condition (c), both the anodic current density and cathodic current density were steady with time, indicating the formation of a flat and smooth alloy layer. As discussed above, excessive anodic dissolution of a substrate should be avoided for flat and smooth alloy surfaces, and it was found that the current density transients could distinguish the dissolution circumstance. A flat and continuous iron-chromium layer was obtained also on the 0.2 mass%C and 0.6 mass%C steel substrates under the conditions; $E_c = -1.1$ V, $E_a = -0.1$ V, $t_c = 4.00$ s, and $t_a = 0.25$ s as shown in Fig. 12.

Figure 13 shows the surface SEM images of the 0.2 mass%C steel substrates before and after the processing by alternating pulsed electrolysis under the conditions: $E_c = -1.1$ V *vs.* SHE, $E_a = -0.1$ V *vs.* SHE, $t_c = 4.00$ s, and $t_a = 0.50$ s, but different numbers of pulse cycles. The substrate had many original pits on the surface (see Fig. 13(a)). Furthermore, faint patterns due to cementite appeared and many pits still remained on the substrate surface after the pulsed electrolysis with 150 pulse cycles. However, after 900 cycles, those pits were uniformly covered with the deposits, indicating that alternating pulsed electrolysis improved the asperity of the substrate. The chromium content in the deposited layer increased with the increase in pulse cycles as shown in Fig. 14. At the beginning of the pulsed electrolysis, an iron-chromium layer with a low chromium content was formed on the surface, and it was repeatedly deposited and dissolved, resulting in irregularity of the surface. The substrate surface was then gradually covered with a hardly soluble iron-chromium layer which had a high chromium content and the substrate surface became flat and uniform.

4. Conclusions

In this work, the applicability of alternating pulsed electrolysis was examined for the surface alloying of carbon steels with carbon contents of 0.2 mass%, 0.6 mass%, and 0.8 mass%. Before the pulsed electrolysis, the dissolution

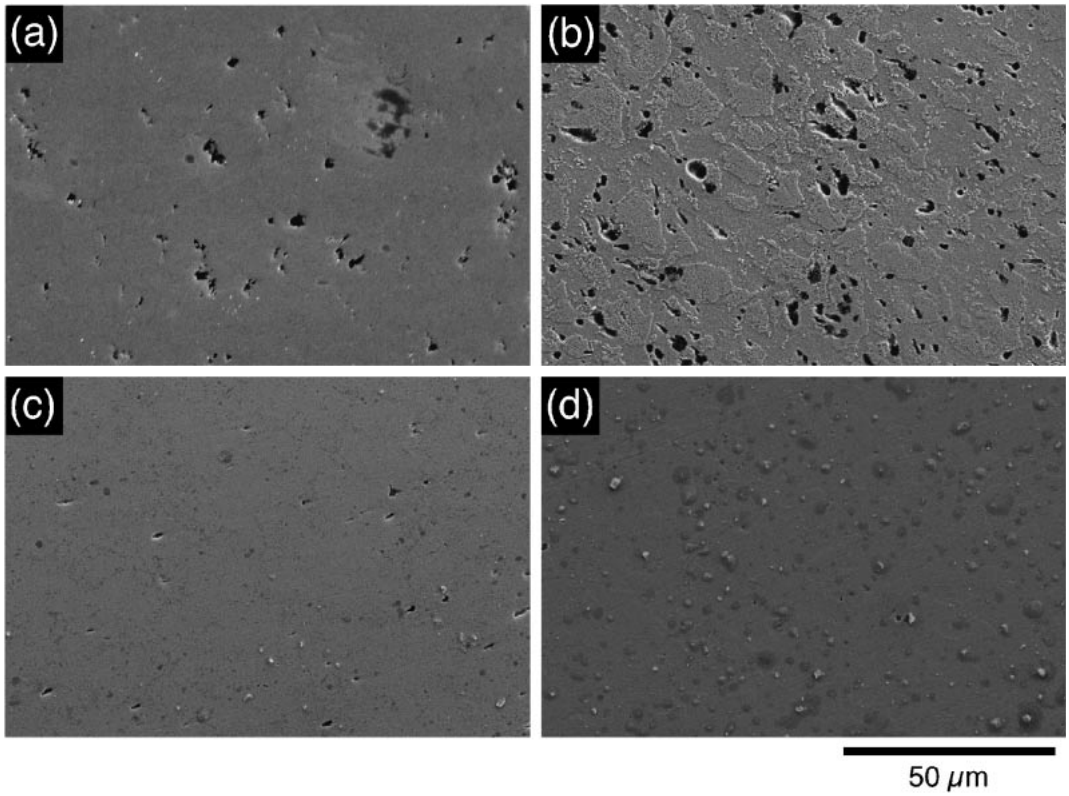

Fig. 13 Surface SEM images of 0.2 mass%C steel substrates processed by alternating pulsed electrolysis for (a) 0 pulse cycles (before processing), (b) 150 pulse cycles, (c) 450 pulse cycles, and (d) 900 pulse cycles under the conditions: $E_c = -1.1$ V *vs.* SHE, $E_a = -0.1$ V *vs.* SHE, $t_c = 4.00$ s, and $t_a = 0.50$ s in an aqueous solution (pH 2.4) containing 0.10 kmol m^{-3} $Cr_2(SO_4)_3$, 1.0 kmol m^{-3} KCl, 0.65 kmol m^{-3} H_3BO_3, 1.0 kmol m^{-3} NH_4Cl, and 1.0 kmol m^{-3} HCOOK.

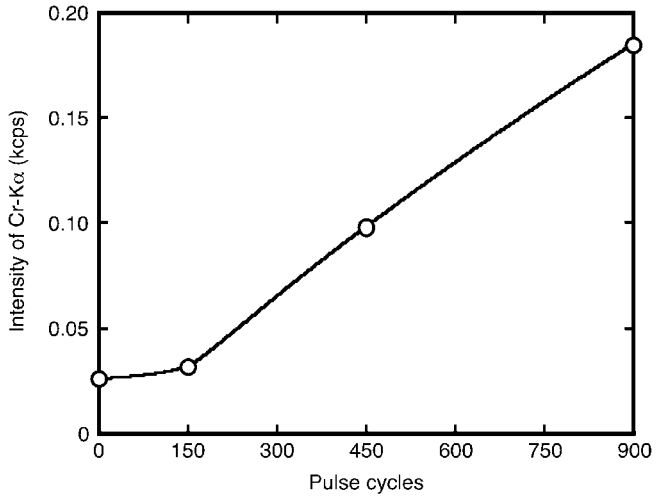

Fig. 14 Cr-Kα intensities of layers formed on 0.2 mass%C steel substrates by alternating pulsed electrolysis from an aqueous solution (pH 2.4) containing 0.10 kmol m^{-3} $Cr_2(SO_4)_3$, 1.0 kmol m^{-3} KCl, 0.65 kmol m^{-3} H_3BO_3, 1.0 kmol m^{-3} NH_4Cl, and 1.0 kmol m^{-3} HCOOK under the conditions: $E_c = -1.1$ *vs.* SHE, $E_a = -0.1$ V *vs.* SHE, $t_c = 4.00$ s, $t_a = 0.50$ s, and 0–900 pulse cycles.

behavior of pure iron and carbon steels was investigated in the solution. Pure iron was easily dissolved at a potential of 0.0 V *vs.* SHE and left a uniform surface macroscopically. However, the surface was not uniform microscopically, showing close-packed planes of bcc iron, *i.e.* 110 planes. On the other hand, the ferrite phase of carbon steel was easily dissolved, but the cementite phase was difficult to dissolve, resulting in nonuniform dissolution of the surface. The nonuniform dissolution of carbon steel affected the formation of the iron-chromium alloy layer by alternating pulsed electrolysis. The alloy layer tended to peel off from the substrate processed even under the same conditions as that under which the flat and continuous layers were obtained on the pure iron substrate. However, flat and smooth alloy layers were obtained by reducing the amount of dissolved iron during each anodic pulse, and alternating pulsed electrolysis improved the asperity of the substrate.

Acknowledgments

The present work was supported by the Kyoto University 21st Century COE Program, "United Approach to New Materials Science," from the Ministry of Education, Culture, Sports, Science and Technology of Japan.

REFERENCES

1) G. Dubpernell: Plating **47** (1960) 35.
2) M. Kishi: Hyomen Gijutsu **37** (1986) 159.
3) G. J. Sargent: Trans. Am. Electrochem. Soc. **37** (1920) 479.
4) G. R. Davies: Electroplat. Metal Finish. **21** (1968) 3.
5) S. Konishi and M. Tadagoshi: Hyomen Gijutsu **23** (1972) 585.
6) S. Eguchi and T. Yoshida: Hyomen Gijutsu **33** (1982) 272.
7) M. Selvam: Metal Finish. **81** (1983) 37.
8) T. Morikawa and S. Eguchi: Hyomen Gijutsu **37** (1986) 341.
9) J. C. Saiddington and G. R. Hoey: Plating **61** (1974) 923.

10) J. C. Saiddington: Plat. Surf. Finish. **65** (1978) 45.
11) T. A. Eckler, B. A. Manty and P. L. McDaniel: Plat. Surf. Finish. **67** (1980) 60.
12) M. H. Gelchinski, L. Gal-Or and J. Yahalom: J. Electrochem. Soc. **129** (1982) 2433.
13) T. Hirato, T. Terabatake, E. Watanabe and Y. Awakura: Hyomen Gijutsu **47** (1996) 245.
14) J. C. Crowther and S. Renton: Metal Finish. **28** (1975) 6.
15) S. Kato, S. Goto and S. Konishi: Hyomen Gijutsu **28** (1977) 121.
16) Y. Mizutani: Hyomen Gijutsu **32** (1981) 86.
17) P. Benaben: Plat. Surf. Finish. **76** (1989) 60.
18) M. El-Sharif and C. U. Chisholm: Trans. Inst. Metal. Finish. **75** (1997) 208–212.
19) S. Yagi, K. Murase, T. Hirato and Y. Awakura: Electrochem. Solid-State Lett. **9** (2006) B32–B34.
20) S. Yagi, K. Murase, T. Hirato and Y. Awakura: J. Electrochem. Soc. **154** (2007) D304–D309.
21) S. Kato, S. Goto and S. Konishi: Hyomen Gijutsu **28** (1977) 121.
22) O. Kubaschewski: Iron - Binary Phase Diagrams, (Springer-Verlag Berlin/Heidelberg, and Verlag Stahleisen mbH, Düsseldorf 1982) pp. 23.
23) T. Taoka, K. Ogasa, E. Furubayashi and S. Takeuchi: J. Japan Inst. Metals **30** (1966) 820.